Observations from Exploration of VTOL Urban Air Mobility Designs

Wayne Johnson **Christopher Silva**

wayne.johnson@nasa.gov christopher.silva@nasa.gov

Ames Research Center, National Aeronautics and Space Administration
Moffett Field, California USA

ABSTRACT

NASA is exploring rotorcraft designs for VTOL air taxi operations, also known as urban air mobility (UAM) or on-demand mobility (ODM) applications. Several concept vehicles have been developed, intended to focus and guide NASA research activities in support of aircraft development for this emerging market. This paper summarizes the work conducted to date. To initially explore the broad design trade-space, three concept vehicles were designed: a quadrotor with electric propulsion; a side-by-side helicopter with hybrid propulsion; and a tiltwing with turbo-electric propulsion. Next a specific UAM mission was developed, accounting for the existing geography, population patterns, infrastructure, and weather in twenty-eight markets across the United States of America. Then in order to quantify the tradeoffs and performance targets necessary for practical implementation of the UAM vision, aircraft were designed to perform this mission, considering a range of aircraft types and propulsion system architectures: quadrotor aircraft, with turboshaft and all-electric propulsion; side-by-side aircraft, with turboshaft and all-electric propulsion; and lift+cruise aircraft with all-electric and turbo-electric propulsion. In examining these vehicles, performance targets and recurring technology themes emerged, which can guide investments in research and development within NASA, other government agencies, academia, and industry. In addition, results from the designs support observations about the trade-offs and key design decisions.

INTRODUCTION

Urban air taxi operations, also known as urban air mobility (UAM) or on-demand mobility (ODM) applications, are enabled by vertical take-off and landing (VTOL) capability. The power and energy requirements of VTOL aircraft are minimized by using low disk-loading rotors, and requiring only short range permits consideration of non-traditional propulsion concepts. The community of innovation has recognized that technology advances in structures, automation and control, energy generation-storage-utilization, and tools for design and analysis, coupled with pressures of resource availability and population density, make this the right time to explore new ways to move people and goods.

The NASA Revolutionary Vertical Lift Technology project (RVLT) has been developing tools and datasets to support the design of advanced vertical lift aircraft. In the last few years, this work has focused on the development of multidisciplinary tools for design and optimization of aircraft with low emissions and low acoustics as objectives. These tools and processes are now also being applied to the new design challenges brought by UAM requirements.

Presented at the 7th Asian/Australian Rotorcraft Forum, Jeju Island, Korea, October 30–November 1, 2018.

The NASA RVLT project is developing UAM rotorcraft designs (Refs. 1–4) that can be used to focus and guide research activities in support of aircraft development for emerging aviation markets. These NASA concept vehicles encompass relevant technologies (including battery, hybrid, internal-combustion propulsion, distributed electric propulsion, highly efficient yet quiet rotors), although it is desirable that NASA designs are different in appearance and design detail from prominent industry arrangements. The design work also provides a context for developing design and analysis tools.

This paper summarizes the results of these recent NASA investigations, which was conducted in several phases: reduced-emission rotorcraft concepts; concept vehicles for air taxis operations; and vehicles for the UAM mission. The software tool suite used is outlined, and the concept aircraft developed in each phase are described. Observations about the design trade-offs and key design decisions are discussed.

DESIGN AND ANALYSIS TOOLS

A goal of the present tool suite development effort within NASA's RVLT project is to provide robust computational methods that facilitate design space exploration with varied problem definitions and with the ability to concurrently consider several different potential solutions. A second goal is to speed the setup and execution of design space exploration, specifically for vertical lift aircraft designed to objective functions other than

minimization of acquisition or operating cost. Conceptual design tools are constructed with flexibility to design and analyze a large variety of aircraft, yet many of the underlying empirical models are limited by their basis in historic aircraft data. A solution to this limitation is to separate the design and analysis procedures into those which are performed by the monolithic design tool and those which are performed by interconnected tools which are capable of returning results for their domain of applicability with the information available at the conceptual design stage.

The tool suite used encompasses the following software:

a) Conceptual design: NDARC (NASA Design and Analysis of Rotorcraft, Refs. 5–8).
b) Execution environment and optimization: OpenMDAO and RCOTools (Ref. 9).
c) Aircraft and rotor acoustics: ANOPP/ANOPP2 and AARON (Refs. 10–11).
d) Engines: NPSS (Ref. 12).
e) Handling qualities and control, analysis and assessment: SIMPLI-FLYD (Ref. 13).
f) Blade and wing structure design and analysis: IXGEN and UM-VABS (Ref. 14).
g) Geometry: OpenVSP and ALPINE (initial geometry, Refs. 15–16), Rhino (final geometry).
h) Aeromechanics: rotorcraft comprehensive analysis CAMRAD II (Refs. 17–18).

NDARC has a modular architecture, facilitating its application to new aircraft and propulsion types, including non-traditional propulsion systems (Ref. 8). CAMRAD II was used in the optimization of the rotor geometry for the aircraft sizing conditions, and to develop calibrated rotor performance models for NDARC; as well as to calculate rotor and hub loads for structural design, assess rotor and blade stability and whirl flutter, and provide rotor blade airloads for mid-fidelity acoustics calculations.

REDUCED-EMISSION ROTORCRAFT CONCEPTS

RVLT's recently concluded investigation focused on the development of an integrated tool suite for the multidisciplinary design and optimization of VTOL aircraft for reduced emissions and acoustics (Ref. 1). Rotorcraft concepts were developed with the goal of producing less than 50% of the climate-impacting emissions of today's fielded technology. NDARC has two models for emissions (Ref. 5): the emissions trading scheme (ETS) of the European Union, which accounts for CO_2 only (metric is kg CO_2 per mission); and the average temperature response (ATR), which captures long-time integrated effects of CO_2, H_2O, NO_x, O_3, CH_4, SO_4, soot, and aviation induced cloudiness (metric is nano-°C of warming per mission). For electric propulsion, the ETS method includes the CO_2 produced in generating the energy. For turboshaft propulsion, the ATR method uses an engine NO_x emission model.

Figure 1 shows the three size classes considered, and the baseline vehicles: single-main-rotor and tail-rotor helicopters for classes A and B, and a tiltrotor for class C. The baseline represents today's technology (TRL 9): un-faired hubs and aluminum structure for helicopters; fly-by-wire and fastened composites for tiltrotors; current technology turboshaft engines; crashworthy structures; and inclement weather operation.

Class A: 5 passengers + pilot, 400 nm range

Class B: 24 passengers + 3 crew, 500 nm range

Class C: 76 passengers + 5 crew, 1300 nm range

Figure 1. Reduced-emission rotorcraft concepts: size classes and baseline vehicles.

Figure 2 shows the reduced-emission rotorcraft designs. The principal characteristics of the baseline and reduced-emission designs are given in table 1. While several advanced aircraft types were considered (figure 2), table 1 only presents the baseline and the best (lowest-emission) designs for each class. Advanced technologies (TRL 5+) considered include more attention to drag (faired hubs, landing gear), more composite structures (bonded instead of fastened), advanced drive systems materials and approaches, and advanced turboshafts for classes B and C. These technologies alone could not make the helicopters clean enough, with only about 20% reduction in emissions for class A, and 35–40% reduction for classes B and C. Considering more efficient aircraft types was necessary: coaxial helicopters, side-by-side helicopters, and high efficiency civil tiltrotors (HECTR). The HECTR design for class C achieved 70% reduction of emissions. The side-by-side helicopter (2 or 4 rotors) and the HECTR achieved 65% reduction of emissions for class B. The lack of an efficient small (<1000 shp) turboshaft development meant that turboshaft-power designs for class A did not

achieve the goal: 20% reduction of emissions for the single main-rotor and tail-rotor helicopter, 30% reduction for the coaxial helicopter or tiltrotor. The tiltrotor does not get light enough to take advantage of its cruise efficiency.

Electrical propulsion concepts were examined for the smaller classes, considering very long-term goals for weights and efficiencies (currently below TRL 2). Battery-powered aircraft do not meet the goal, since besides increasing the vehicle weight, U.S. electric grid emissions are high. Emissions from fuel cells can be very low, even if the hydrogen is obtained from a methane source, although the weights are high.

This work on low-emission rotorcraft provided the foundation for exploring UAM designs: development of an integrated tool suite for the multidisciplinary design and optimization of VTOL aircraft; demonstration of alternate propulsion architectures in NDARC, including electric power; and quantification of the cruise efficiency of the side-by-side helicopter type.

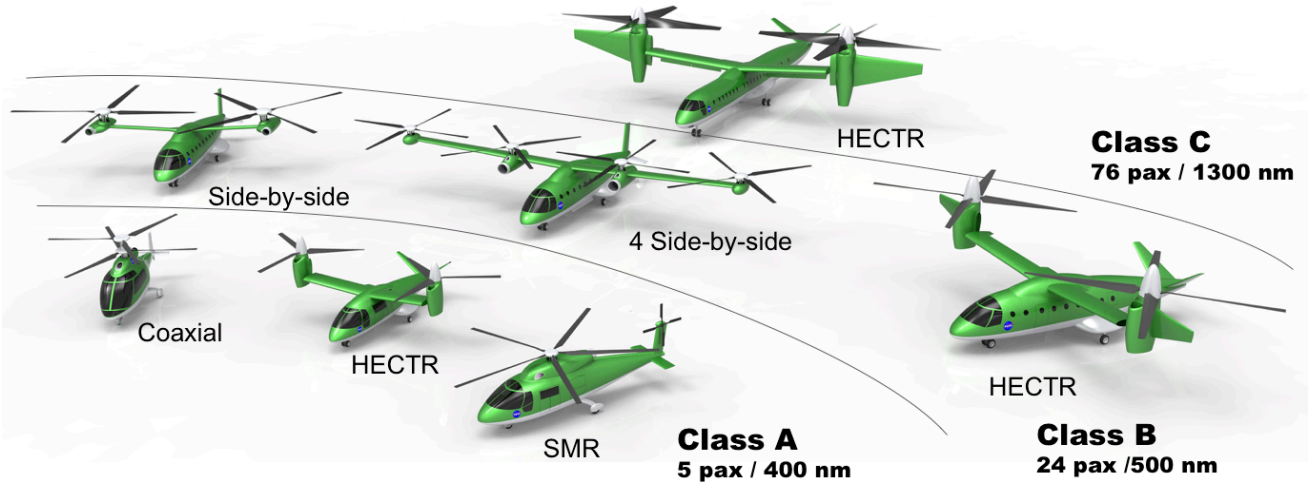

Figure 2. Reduced-emission rotorcraft concepts: environmentally-friendly aircraft designs.

Table 1. Characteristics of reduced-emissions aircraft.

		Single Main-Rotor	Coaxial	Single Main-Rotor	Side-by-Side	Tiltrotor	HECTR
		baseline	low emission	baseline	low emission	baseline	low emission
Payload	lb	1000	1000	5280	5280	16500	16500
Range	nm	400	400	500	500	1300	1300
Rotor Radius	ft	15.2	13.7	29.6	23.2	27.8	26.5
Disk load	lb/ft^2	8.0	8.0	9.0	6.0	20.0	15.7
Power	hp	1070	766	9829	3300	31586	23722
DGW	lb	5781	4586	36402	20223	135260	69163
Empty Weight	lb	3597	2694	23942	11906	90248	40729
Fuel burn	lb	855	594	5732	2021	25763	8880
ETS	kg CO_2	1637	1141	10897	3835	46222	16287
ATR	nano°C	10.4	7.3	68	24	314	110
Emissions Reduction	%		–30%		–65%		–65%

CONCEPT VEHICLES FOR AIR TAXI OPERATIONS

To begin the process of developing concept vehicles for air taxi operations, the range of aircraft attributes being considered by the design community was examined:

a) number of occupants (including pilot): 1, 2, 4, 6, 15, 30;
b) un-refueled range: 50, 100, 200, 400, 800 nm (as multiples of 50 nm segments for this investigation);
c) market: air taxis, commuter scheduled, mass transit, airline;
d) aircraft type: multicopter, side-by-side, tiltwing, tiltrotor, lift+cruise, vectored thrust, compound, helicopter;
e) propulsion system: turboshaft, turbo-electric, electric, parallel hybrid, fuel cell, diesel.

NASA developed three concept vehicles (Ref. 2) that encompass many elements of this design space:

1) A single-passenger (250-lb payload), 50-nm range quadrotor with electric propulsion (figure 3), using flapping rotors and collective control; design excursions included rigid rotors, rotor speed control (fixed pitch blades), and reciprocating engines.
2) A six-passenger (1200-lb payload), 4x50 = 200-nm range side-by-side helicopter with hybrid propulsion (figure 4).
3) A fifteen-passenger (3000-lb payload), 8x50 = 400-nm range tiltwing with turbo-electric propulsion (figure 5), using four propellers with collective and cyclic control; design excursions included tail propellers for pitch and directional control.

The principal characteristics of these concept aircraft are given in table 2.

The primary sizing mission consists of the following segments: (1) 2 min hover out-of-ground-effect (OGE) for takeoff; (2) fly 50 nm at best-range speed; (3) 2 min hover OGE for landing; (4) fuel/energy reserve minimum of 10% of mission or 20 min flight at best-endurance speed. All the segments are flown at atmospheric conditions of 5000-ft altitude and ISA+20°C temperature. Segments 1–3 are repeated for each 50 nm leg in the un-refueled range. Cruise is flown at best-range speed (99% high side), unless the maximum speed is less than V_{br}. Reserve requirements are based on 14 CFR 91.151: 20 min at cruise speed for visual flight rules (VFR) rotorcraft. A second sizing mission has these segments flown at sea level and ISA+20°C temperature.

All-weather operations are assumed, which has an impact on systems weight (including de-icing). For low aircraft noise, the design rotor tip speed is low compared to conventional helicopters: 450 ft/sec for the quadrotor, 550 ft/sec for the larger aircraft. (In general, reducing the design hover tip speed increases the size of the aircraft; the consequences of weight growth are less for a small aircraft, so a lower tip speed can be used for the quadrotor.) Maximum speed (from power available at 90% MCP) is fallout, with installed power determined by takeoff conditions.

Figure 3. Concept aircraft: single-passenger quadrotor with electric propulsion.

Figure 4. Concept aircraft: six-passenger side-by-side helicopter with hybrid propulsion.

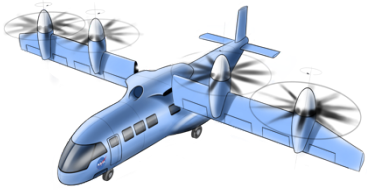

Figure 5. Concept aircraft: fifteen-passenger tiltwing with turboelectric propulsion.

Table 2. Characteristics of concept aircraft.

aircraft		Quadrotor	Side-by-Side	Tiltwing
propulsion		electric	hybrid	turbo-electric
Payload	lb	250	1200	3000
Range	nm	50	200	400
Rotor Radius	ft	6.5	11.8	6.1
Disk load	lb/ft^2	2.5	4.5	30.0
L/D_e = WV/P		5.3	6.0	7.2
Power	hp	4x23	2x187 +100*	4x731 +4730**
DGW	lb	1325	3950	14039
Empty Weight	lb	1070	2390	8918
Structure	lb	394	1050	3495
Propulsion	lb	118	562	3010
Battery	lb	286	103	450

* turboshaft & motor **motor & turboshaft

Approaches to deal with component failures in the propulsion system are needed, but the impact of such failures was only partially accounted for in these concept vehicle designs. For conventional propulsion systems, identifying approaches for safe one-engine inoperative (OEI) flight, including takeoff operations and power requirements, and the requirements for all-engine inoperative (AEI) operations and/or autorotation capability is needed. Similar requirements must be developed for the non-traditional propulsion systems.

VEHICLES FOR THE UAM MISSION

Following the initial air taxi vehicle study, which explored vehicle technology themes using aircraft of various sizes designed for several candidate missions, RVLT performed a focused study to better understand a particular urban air mobility market. A design mission was developed accounting for the existing geography, population patterns, infrastructure, and weather in twenty-eight markets across the United States of America (Ref. 3). The resulting mission is to carry six passengers (including the pilot, if not autonomous; 1200 lb) on two 37.5-nm flights (total 75-nm range without recharging or refueling), with a 20 min reserve (figure 6). Takeoff altitude is 6000-ft (ISA), and cruise is at best range speed, 4000-ft above ground level. This mission is intended to be used as a sizing requirement. The actual operational missions flown by the aircraft will be different, driven by economics, air traffic, and other aspects of a particular flight.

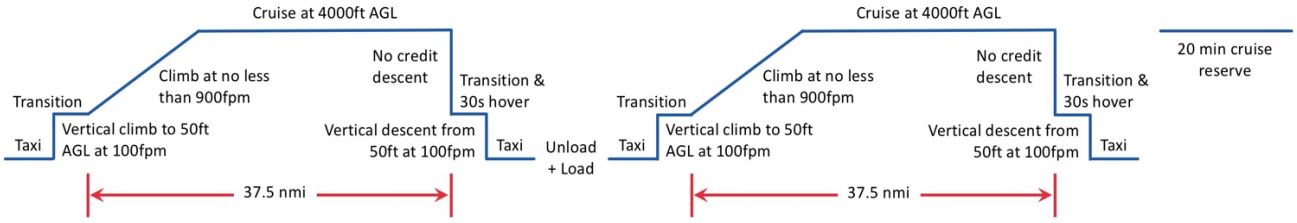

Figure 6. UAM sizing mission profile.

Quadrotor
turboshaft or battery

Side-by-Side Helicopter
turboshaft or battery

Lift+Cruise VTOL
turbo-electric or battery

Figure 7. UAM aircraft designs: six occupants (1200 lb), 75 nm range.

In order to quantify the tradeoffs and performance targets necessary for practical implementation of the UAM vision, six aircraft were designed to perform this mission (Ref. 4). A range of aircraft types and propulsion system architectures were considered: quadrotor aircraft, with turboshaft and all-electric propulsion; side-by-side aircraft, with turboshaft and all-electric propulsion; and lift+cruise aircraft with all-electric and turbo-electric propulsion (figure 7).

Consistent technology assumptions were made to size the vehicles:

a) Battery pack modeled as Li-Ion (TRL 1): installed, usable specific energy 400 Wh/kg (well beyond state-of-the-art); maximum mission current 4C, emergency 14C (high end state-of-the-art).b) Wiring and accessory electric systems as fractions of motor weight (TRL 3).
b) Structures (TRL 3+): composite VTOL structures, very lightweight booms.
c) Aerodynamics (TRL 5+): passive rotor and airframe lift/drag.
d) Propulsion (TRL 5+): high torque/weight electric motors; high torque/weight transmissions.
e) Systems (TRL 5+): equipment for instrument flight rules (IFR) operations (hence autonomy possible without additional weight); environmental control systems, insulation, seating.

All six aircraft (three aircraft types, two propulsion architectures for each) were designed to the same mission. The principal characteristics of the designs are given in table 3. Figure 8 shows the range of cruise efficiency

(L/D_e = WV/P) and hover efficiency (W/P) of these designs. For reference, L/D_e of 5 is achieved by very efficient helicopters, and a rather efficient fixed-wing general aviation aircraft (Cirrus SR22T) is shown at its best-range L/D_e = 10 at 10000 ft/ISA and maximum gross weight. Thus these VTOL aircraft are more efficient than helicopters in cruise, and are approaching the efficiency of a good fixed-wing aircraft flying at moderate altitudes. Hover efficiency depends on hover disk loading, which is optimized to minimize size for each aircraft. The overlapped rotors of the side-by-side helicopter give it good span efficiency, resulting in good cruise efficiency. The lift+cruise aircraft cruises with the lift rotors stopped, increasing the L/D_e. Figure 9 shows the breakdown of the weight empty. For each design, the payload is 1200 lb and the fuel for turboshaft propulsion is 150–180 lb. Generally, structural and propulsion weights increase with the number of rotors. There is only one design mission, so the battery capacity equals the energy (including reserve) needed for that mission. Even high specific-energy batteries are heavy, so all-electric propulsion produces a heavier aircraft than turboshaft or hybrid propulsion. The high cruise efficiency of the lift+cruise type reduces the battery weight compared to the quadrotor, but not enough to counter the increase in structure and propulsion weight, so the all-electric lift+cruise aircraft is the largest design.

Table 3. Characteristics of UAM aircraft.

	aircraft	Quadrotor	Quadrotor	Side-by-Side	Side-by-Side	Lift+Cruise	Lift+Cruise
	propulsion	turboshaft	electric	turboshaft	electric	turbo-electric	electric
Payload	lb	1200	1200	1200	1200	1200	1200
Range	nm	75	75	75	75	75	75
Rotor Radius	ft	9.2	13.1	10.5	14.9	5.0	5.0
Disk load	lb/ft^2	3.5	3.0	5.0	3.5	8.6	10.9
L/D_e		4.9	5.8	5.9	7.2	7.6	9.3
Power	hp	2x305	4x168	2x232	2x214	8x96+412*	8x136+538*
DGW	lb	3735	6480	3468	4897	5943	7517
Empty Weight	lb	2345	5270	2111	3687	4567	6308
Structure	lb	1101	1641	940	1235	2031	2301
Propulsion	lb	554	11001	522	690	1363	1395
Battery	lb		1561		993	194	1447

*lift motors & cruise motor

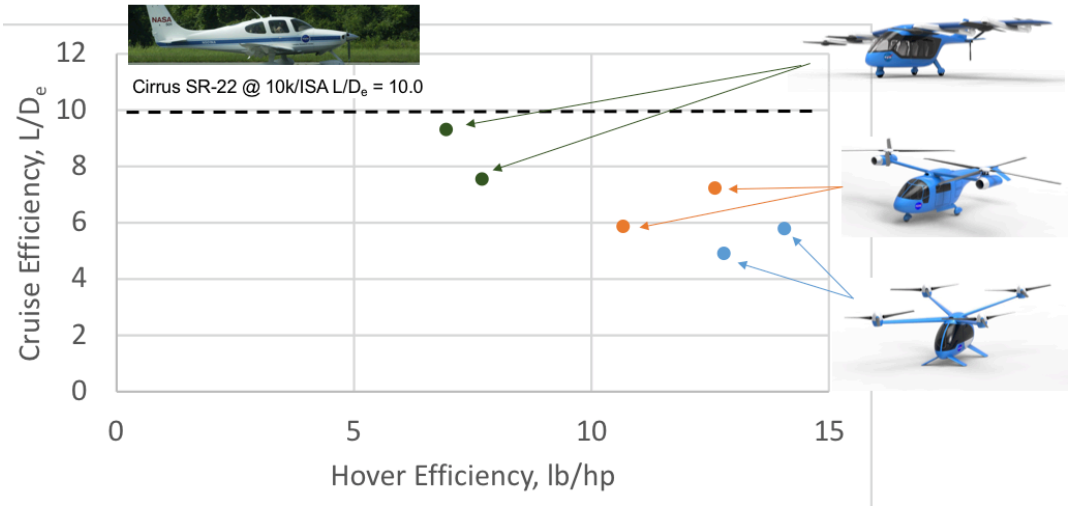

Figure 8. Cruise and hover aerodynamic efficiencies of UAM designs (L/D_e=WV/P).

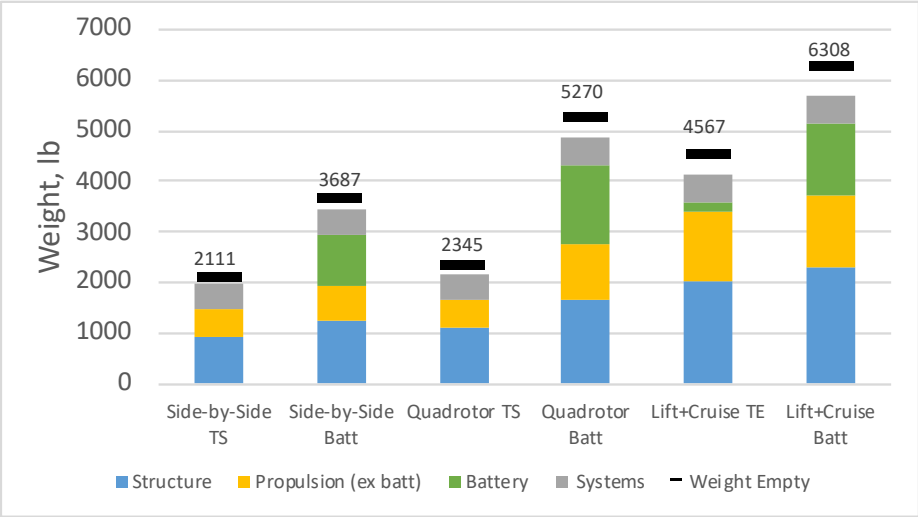

Figure 9. Structure, propulsion, and systems components of empty weight (TS = turboshaft, TE = turbo-electric; weight empty = structure + propulsion + systems + vibration control + contingency).

OBSERVATIONS

In examining the vehicles from this series of design investigations, performance targets and recurring technology themes emerged, which may guide investments in research. In addition, results from the various designs support observations about the trade-offs and key design decisions.

Noise and Annoyance

The UAM vehicles have been designed with low hover tip speed (450 ft/sec for the single-passenger quadrotor, 550 ft/sec for the other aircraft), in anticipation of a significant requirement for noise reduction in the urban environment. Rotor-rotor interactions, such as rear rotors operating in the wake of front rotors, and wake interactions on retreating sides of overlapped side-by-side rotors, will increase blade-vortex interaction noise. Blade shape and spacing can be optimized for low blade-vortex-interaction and high-speed-impulsive noise.

Noise metrics and requirements are established by regulation for rotorcraft, but suitability and applicability of these to air taxi operations must be established. Possibly new metrics will be required, and the new requirements may not be met by simply using low tip-speed rotors. Active control of rotor noise can achieve significant noise reductions, with 6 to 12 dB reduction demonstrated through analysis, wind tunnel test, and flight test of rotors (Ref. 19).

For the low-emission concept vehicles, rotor noise has been calculated, and design features devised to reduce noise for FAA-defined flight conditions. Work is presently underway in RVLT to perform similar acoustic analysis and design work for the UAM vehicles.

Safety and Airworthiness

Airworthiness approval means a document, issued by the FAA for an aircraft, which certifies that the aircraft conforms to its approved design and is in a condition for safe operation (14 CFR 21.1(b)(2)). While certification requirements and procedures for air taxi aircraft may be debated, negotiated, or even contested, for aeromechanics research the focus is on safe operation. Every innovative aircraft type and non-traditional propulsion system requires an extensive failure mode, effects, and criticality analysis (FMECA). Important for air taxi aircraft are crashworthiness and the consequences of propulsion system failure. Crashworthiness requirements affect design of airframe structure, landing gear, and passenger accommodation and restraint. Propulsion system failures must be considered in detail. In particular, single as well as complete engine failure must be considered, with requirements for control and methods for safe landing.

In these concept vehicles, degraded weather operation, propulsion system failures, and crashworthiness have been assumed to be requirements, and technology factors representing these design considerations have been applied. Work is presently underway in RVLT to further analyze the UAM vehicles for these safety and airworthiness considerations.

Cost

Purchase cost of aircraft is roughly (20% accuracy) driven by aircraft empty weight, installed power, and complexity, plus the costs of electronic systems. For electric propulsion, the cost of batteries should be explicitly included in the purchase cost estimate.

Data are available for maintenance cost of helicopters flying traditional missions, but not for unconventional aircraft types engaged in air taxi operations.

A significant component of operating costs is the cost of fuel or energy. If the mission range is small enough so that electric propulsion is feasible, energy costs are generally smaller for the all-electric propulsion configuration, even though the aircraft weight is larger.

Battery Technology

The most important factor in the feasibility of electrical propulsion systems is the requirement for light-weight, high-power batteries. The baseline designs here assume an installed, usable specific energy of 400 Wh/kg. Current state-of-the-art batteries have installed specific energy of 100–150 Wh/kg. The weight and power variation with range and battery technology are shown in figure 10 for an electric side-by-side aircraft. High specific energy enables a useful range with a reasonable aircraft weight and power. Aircraft size does not change the conclusions from these figures, as similar results are obtained for both single-passenger and fifteen-passenger side-by-side designs.

The power capability of batteries is also important. High power is obtained with high current, and current can be characterized by fraction x of the charge capacity C: $I = xC$, with units of 1/hr for x. A maximum burst discharge current of 10C to 30C (fully discharged in 6 to 2 minutes) is possible for emergency use, but long battery life typically requires currents of 1C to 3C. The discharge current variation with range is shown in figure 10 for the electric side-by-side aircraft. The cruise current is less than the hover current for these designs, since cruise speed is fallout and the power is sized by the hover condition. The battery capacity is the sum of hover, cruise, and reserve requirements:

$$E_{\text{cap}} = E_{\text{cruise}} + E_{\text{hover}} + E_{\text{reserve}}$$

Writing cruise power in terms of the aircraft effective lift-to-drag ratio ($P_c = WV/(L/D_e)$), the cruise energy is proportional to range:

$$E_{\text{cruise}} = (P_c/\eta_c) \times \text{time} = WV \times \text{time} / ((L/D_e)\ \eta_c)$$
$$= WR / ((L/D_e)\ \eta_c)$$

where η_c is the propulsion system efficiency in cruise, and $R = V \times$ time is the range. From the charge capacity $C_{\text{cap}} = E_{\text{cap}}/v$ (voltage v), and hover current $I = (P_h/v)/\eta_h$ (η_h is propulsion system efficiency in hover), the hover discharge current is

$$x_{\text{hover}} = I/C_{\text{cap}} = P_h/(\eta_h E_{\text{cap}})$$
$$= W\sqrt{W/2\rho A}/FM/(\eta_h E_{\text{cap}})$$

with hover power in terms of figure of merit ($P_h = W\sqrt{(W/2\rho A)}/FM$). Substituting for E_{cap} gives

$$1/x_{\text{hover}} = R\frac{\eta_h FM}{\eta_c (L/D_e)}/\sqrt{W/2\rho A} + \text{constant}$$

where the constant comes from the hover and reserve energy capacity. Ignoring the constant gives

$$x_{\text{hover}} = \sqrt{W/2\rho A}\ \frac{\eta_c (L/D_e)}{\eta_h FM}\ \frac{1}{R}$$

High hover efficiency (low disk loading and high figure of merit) reduces the current, but short range or high cruise efficiency (L/D_e) reduces the battery capacity required, hence increases the hover current x_{hover}. As illustrated in figure 10, this result is independent of battery technology, except as it impacts the range that is achievable by a design. For the side-by-side aircraft, the hover current $x_{\text{hover}} < 1C$ if the range is greater than about 160 nm, $x_{\text{hover}} < 2C$ if the range is greater than about 60 nm.

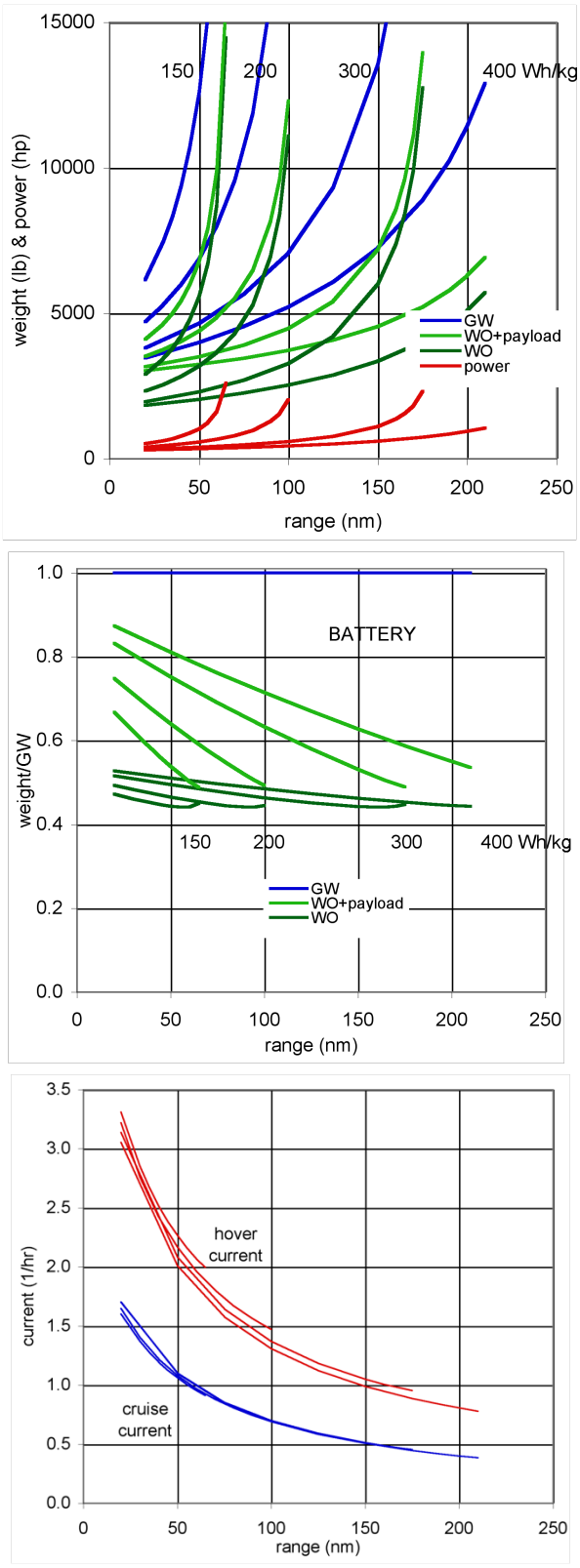

Figure 10. Electric side-by-side helicopter (six passengers): weight and power variation with range and battery technology; discharge current for battery technology 150–400 Wh/kg.

Aircraft Aerodynamic Efficiency

Electric propulsion is enabled by aerodynamic efficiency of the aircraft, in both hover and cruise. For each design, there is a disk loading that minimizes aircraft weight, power, and energy. Small aircraft with edgewise rotors optimize with low disk loading. Rotor-rotor interference must be considered for optimum cruise performance. Interactional aerodynamics impact performance and operation: for tiltwings, wing separation or buffet during conversion must be considered; for tiltrotors, hover download and rotor-tail interactions must be considered. Rotor shape optimization covers blade twist and taper, tip sweep and droop. Drag minimization includes hub, rotor support, and airframe.

For aircraft with two or more main rotors, interactions between the rotors have a significant impact on performance, vibration, noise, and handling qualities. The interactions depend on the arrangement of the rotors. Figure 11 illustrates the wake geometry of the quadrotor and side-by-side aircraft in cruise flight. The overlap of the side-by-side rotors significantly improves the efficiency of cruise flight, because the twin rotors act as a single, large-span wing system. Figure 12 shows the influence of overlap (wing span = 1.0D = rotor diameter means the rotor disks are tangent) on rotor efficiency (rotor $L/D_e=WV/(P_i+P_o)$).

Elevating the rear rotors above the front rotors on the quadrotor reduces the cruise power, as shown in figure 13, by reducing the interference of the wakes of the front rotors on the rear rotors. Elevating the rear rotors is expected to reduce vibration and noise and improve handling qualities as well. Moving the aircraft center of gravity forward of the mid-point between the rotors, so the front and rear rotors trim closer to the same C_T/σ at cruise speed, further reduces the power (figure 13).

The effects of the rotor-rotor interactions may require vibration and load alleviation systems. The present designs have a weight allocation for vibration control.

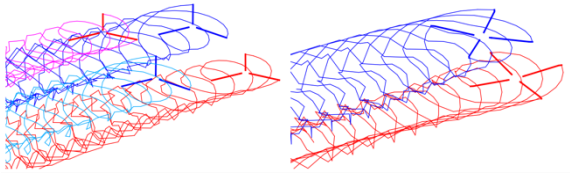

Figure 11. Wake geometry of quadrotor and side-by-side aircraft at cruise speed.

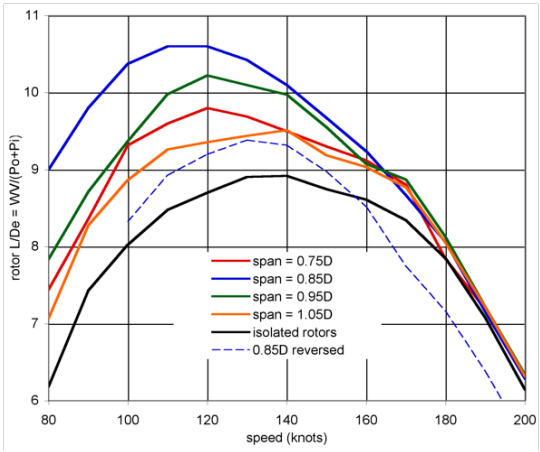

Figure 12. Rotor cruise efficiency as function of overlap for side-by-side helicopter.

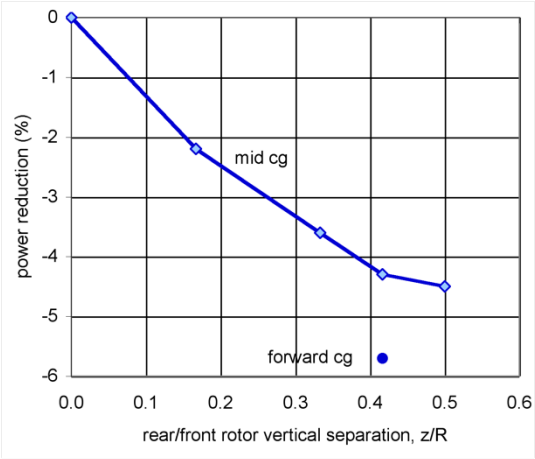

Figure 13. Influence of elevation of rear rotors on cruise performance of quadrotor.

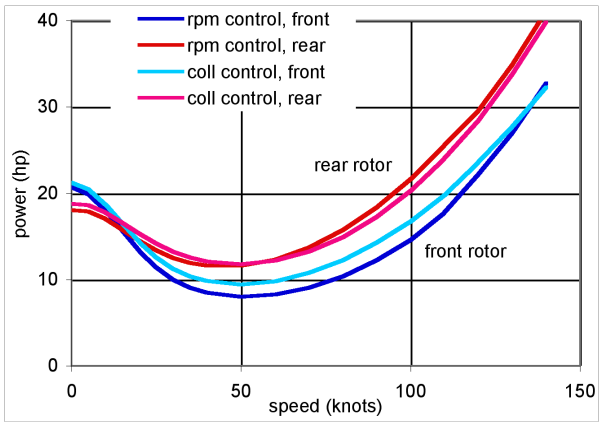

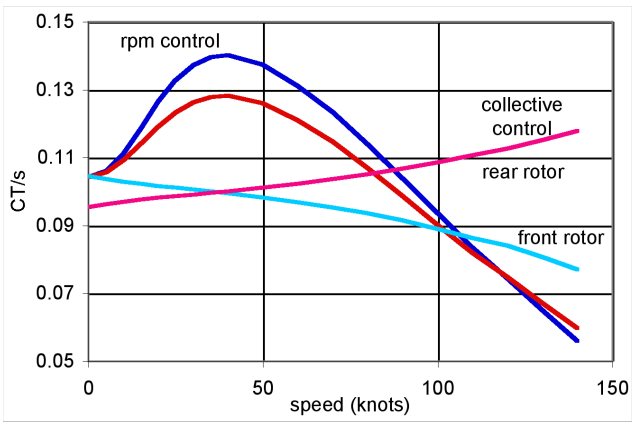

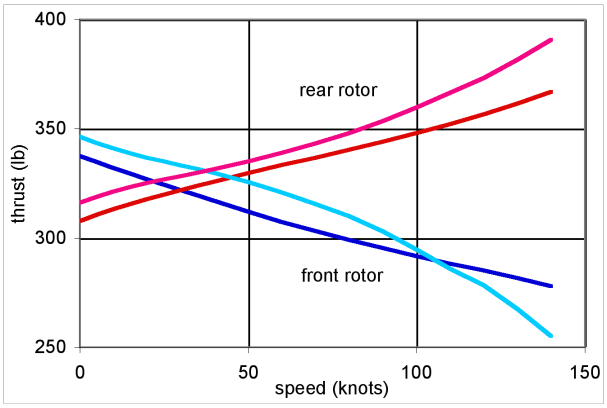

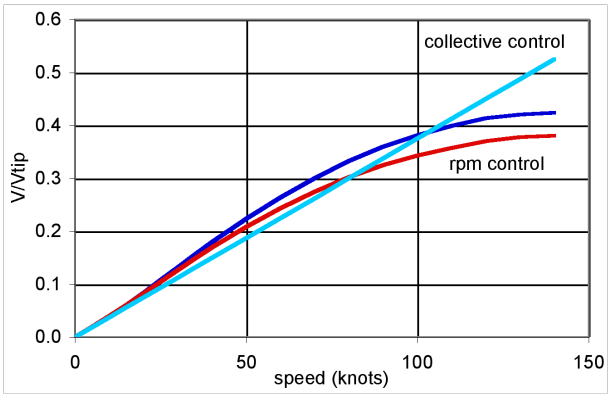

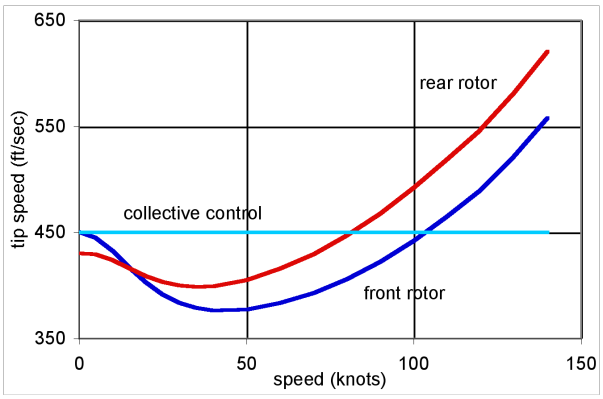

Figure 14. Electric quadrotor trim as a function of flight speed, for collective control and rotor speed control.

Trim of Multi-Rotor Aircraft

For the quadrotor, both collective and rotor speed control were considered. Figure 14 shows the trim operating conditions of the front and rear rotors for the two control methods. Edgewise rotor flight has reduced induced power (relative hover, for the same lift) due to increased flow through the disk, followed by power increasing with speed as the parasite power increases. The thrust of the rear rotors increases with speed relative the front rotors, for aircraft pitch moment trim. With collective control and fixed rotor speed, the rotor C_T/σ follows the thrust variation, remaining moderate, while the collective control follows the power variation with speed. With rotor speed control and fixed collective, the rotor rpm follows the power variation with speed, while the rotor C_T/σ increases with speed initially and then decreases (figure 14). The increase in C_T/σ might be limited by maximum blade loading, perhaps requiring a smaller design C_T/σ at hover (larger solidity).

For the lift+cruise aircraft, figure 15 shows the variation with speed of the rotor blade loading C_T/σ and wing lift coefficient. C_L. This design has rigid rotors for hover and low speed lift, using fixed pitch and rotor speed control. The lift rotors are stopped for cruise, with the wing providing all lift. As the induced power decreases with speed, the rotor blade loading C_T/σ increases. As speed decreases, the wing lift coefficient increases, bringing the wing closer to stall. Figure 15 also shows the rotor loading limits due to stall, measured by maximum thrust, change in thrust derivative with collective, four times the profile power, and twice the profile power. These hingeless, fixed-pitch rotors operate with large hub roll moments in forward flight, here advance ratio 0.36 and lift offset 0.34 at 90 knots, which increases the loading limits due to stall (a flapping rotor has a steady stall limit of about C_T/σ = 0.12 at 90 knots). At sufficiently high speeds (here above 90 knots), blade stall encompasses most of the rotor disk, and the C_T/σ limit decreases. The design hover C_T/σ must be low enough and the wing area large enough, that transition from rotor-borne to wing-borne flight is possible over a reasonable speed range.

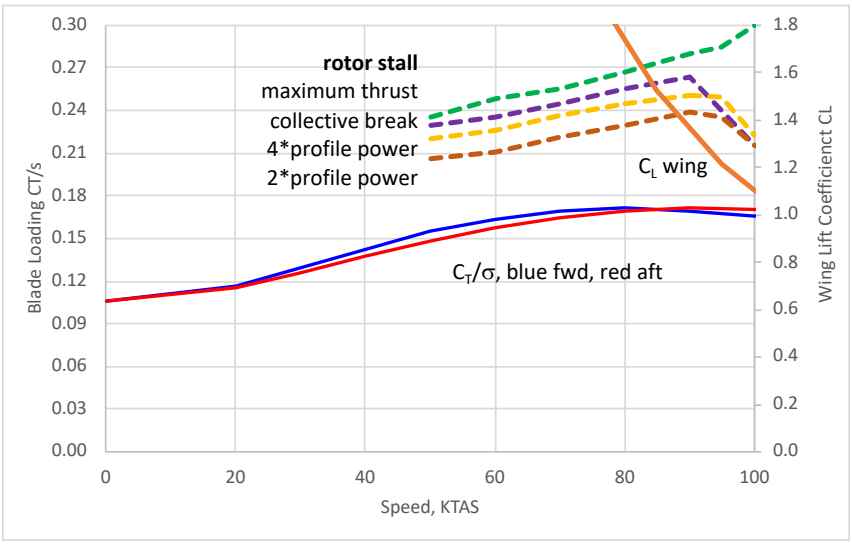

Figure 15. Lift+cruise aircraft rotor blade loading and wing loading variation with speed.

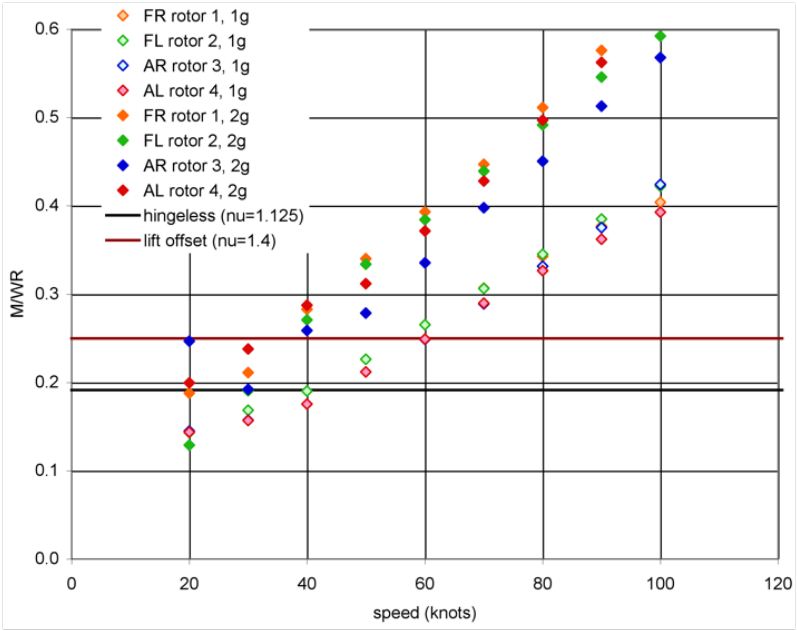

Figure 16. Quadrotor (fixed pitch, hingeless rotors) mean hub moments in level flight and 2g turn.

Rotor/Propeller Design

Design of the rotor or propeller impacts weight, vibration, and handling qualities. For the quadrotor aircraft, both flapping and hingeless rotors were considered. The flapping rotor had 4% hinge offset, with 45° pitch-flap coupling to minimize flapping relative the shaft. The hingeless or rigid rotor generates higher blade and hub loads, hence higher rotor weight and larger weight for vibration control, and the resulting aircraft has 25% larger design gross weight than with flapping rotors.

Figure 16 shows the calculated mean hub moments for the four rotors on the quadrotor aircraft, in level flight and 2g turn. The hub moment is given as lift offset = moment divided by thrust times rotor radius. With no flap hinge and no cyclic pitch, the rotor in edgewise flight operates with increasing lift offset as speed increases. For reference, the design hub moments are shown in figure 16 for typical hingeless rotors (Bo-105 level flap stiffness with 10 deg tip-path plane tilt) and lift offset rotors (design load for 200–250 knot aircraft).

All UAM designs will likely require active control of rotorcraft vibration. Fixed frame active vibration alleviation is common for rotorcraft. In addition, up to 90% reduction of loads and vibration using higher-harmonic control (HHC) or individual blade control (IBC) has been demonstrated through analysis, wind tunnel test, and flight test (Ref. 19).

The UAM designs presented here have technology factors that represent the weight of vibration alleviation systems, excluding HHC or IBC. Work to quantify the payoff and weight of HHC or IBC is beginning for the UAM vehicles, and may result in design changes to improve loads and vibration

Propulsion System Weights

The weight of the motor plus transmission of an electric rotorcraft is shown in figure 17, as a function of rotor radius for a disk loading of 4 lb/ft^2 and tip speed of 550 ft/sec (typical of the present designs). These weights are calculated using parametric equations for motor and drive system weights (Ref. 5), with technology factors appropriate for future designs. N is the motor speed (rpm) for cases with a transmission. For direct drive the motor speed equals the rotor speed. These results show that for current and projected future technology, a high speed (low torque) motor with an advanced transmission is lighter than direct drive. For direct drive to be the lighter design approach, a light weight, high torque motor is required, operating with large mean and oscillatory loads from the rotor.

Figure 18 shows the motor plus transmission weight variation with number of rotors, for a disk loading of 4 lb/ft^2, tip speed of 550 ft/sec, and aircraft weight 5000 lb.

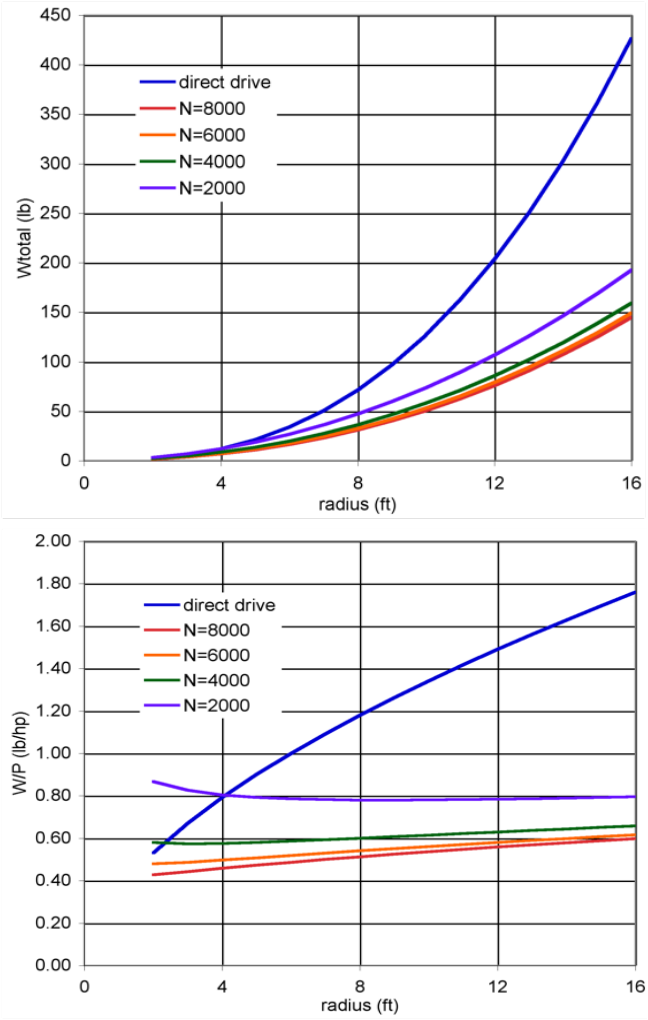

Figure 17. Motor+transmission weight variation with rotor size and motor speed.

Figure 19 adds the rotor weight to the motor and transmission weight, for design C_T/σ = 0.10 and flap frequency of 1.25/rev (typical of hingeless helicopter rotors). The rotor weight is calculated using parametric equations (Ref. 5), which are based on data that includes aircraft weights and rotor diameters corresponding to these designs. Considering just the propulsion system (motor, transmission, and rotor), the weight decreases significantly as the number of rotors increases. Similar results are obtained considering turboshaft engines instead of electric motors. This result is therefore not consistent with the observation that for helicopter designs the single-main-rotor configuration (even with a tail rotor) is preferred to tandem or side-by-side aircraft types. Usually, adding the weight and drag of the structure that supports the rotors changes the optimum solution. Figure 20 shows the empty weights for the three electric-propulsion aircraft designed for the UAM mission. With eight lifting rotors, the lift+cruise type has higher structural weight even though it has the best cruise efficiency.

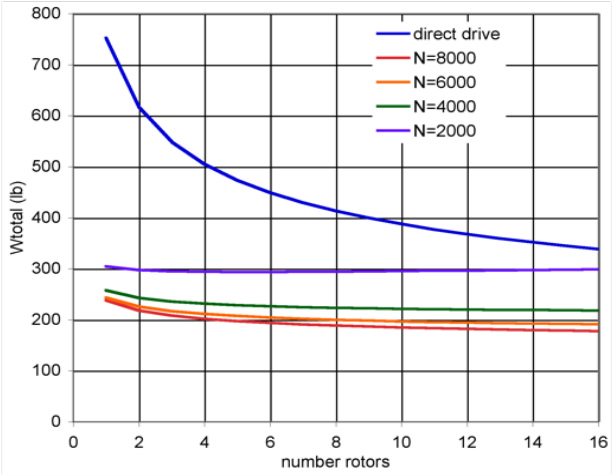

Figure 18. Motor+transmission weight variation with number of rotors and motor speed.

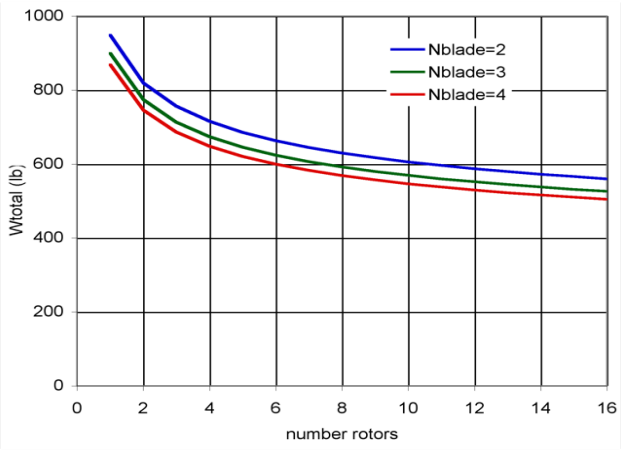

Figure 19. Motor+transmission+rotor weight variation with number of rotors and number of blades.

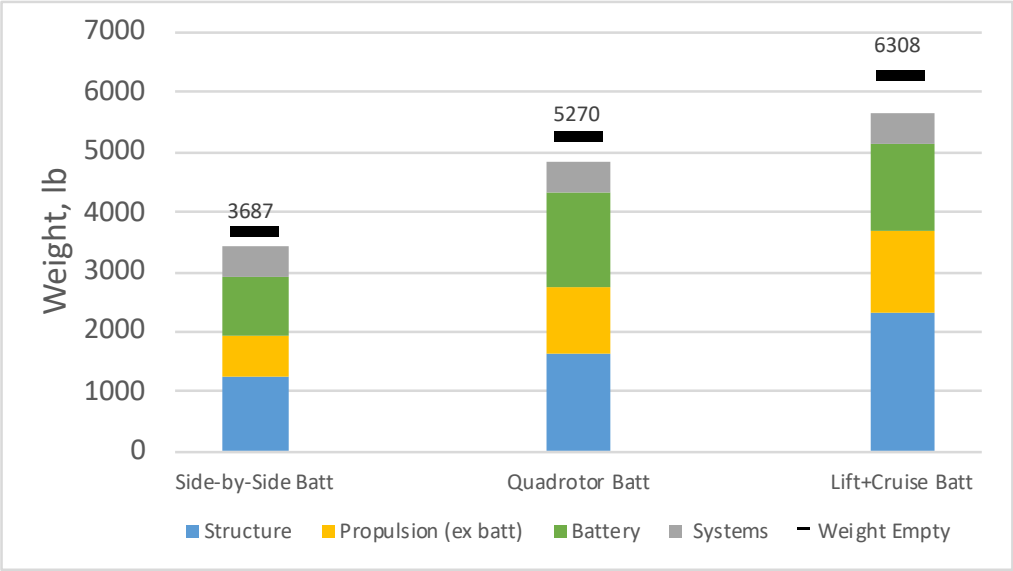

Figure 20. Aircraft empty weight variation with number of rotors.

Assessment of Tools and Data

The design investigations summarized here have demonstrated that the computational tools available for rotorcraft aeromechanics analysis and design are generally applicable to VTOL air taxi aircraft. These tools include comprehensive analyses, computational fluid dynamics codes, rotor and airframe structural analyses, and acoustic codes.

To support design results, component design methods and data bases for unconventional aircraft propulsion systems are required, particularly for electrical subsystems.

The reliability of computational methods used in the design process rests on correlation of results with measured data for relevant aircraft types, systems, and components. Thus data from ground, wind tunnel, and flight tests are needed to substantiate the aeromechanics analysis capability for urban air mobility aircraft.

CONCLUDING REMARKS

NASA is exploring rotorcraft designs for VTOL air taxi operations, also known as urban air mobility (UAM) or on-demand mobility (ODM) applications. Several concept vehicles have been developed, intended to focus and guide NASA research activities in support of aircraft development for this emerging market. This paper has summarized the work conducted to date.

To initially explore the broad design trade-space, three concept vehicles were designed: a quadrotor with electric propulsion; a side-by-side helicopter with hybrid propulsion; and a tiltwing with turbo-electric propulsion. Next a specific UAM mission was developed, accounting for the existing geography, population patterns, infrastructure, and weather in markets across the United States of America. The resulting mission is to carry six passengers (including the pilot, if not autonomous) on two 37.5 nm flights (total 75 nm range without recharging or refueling), with a 20 min reserve. Then in order to quantify the tradeoffs and performance targets necessary for practical implementation of the UAM vision, aircraft were designed to perform this mission. A range of aircraft types and propulsion system architectures was considered: quadrotor aircraft, with turboshaft and all-electric propulsion; side-by-side aircraft, with turboshaft and all-electric propulsion; and lift+cruise aircraft with all-electric and turbo-electric propulsion.

In examining these vehicles, performance targets and recurring technology themes emerged, which can guide investments in research and development within NASA, other government agencies, academia, and industry. Based on these aircraft (and numerous excursions), the research requirements for UAM aircraft development have been identified (figure 21). Within these broad research areas, the NASA Revolutionary Vertical Lift Technology project is focusing on noise and annoyance, safety and airworthiness, all-weather capability, and passenger acceptance.

REFERENCES

1) Silva, C.; Johnson, W.; and Solis, E. “Multidisciplinary Conceptual Design for Reduced-Emission Rotorcraft.” American Helicopter Society Technical Conference on Aeromechanics Design for Transformative Vertical Flight, San Francisco, CA, January 2018.

2) Johnson, W.; Silva, C.; and Solis, E. “Concept Vehicles for VTOL Air Taxi Operations.” American Helicopter Society Technical Conference on Aeromechanics Design for Transformative Vertical Flight, San Francisco, CA, January 2018.

3) Patterson, M.D.; Antcliff, K.R.; and Kohlman, L.W. “A Proposed Approach to Studying Urban Air Mobility Missions Including an Initial Exploration of Mission Requirements.” American Helicopter Society 74th Annual Forum, Phoenix, AZ, May 2018.

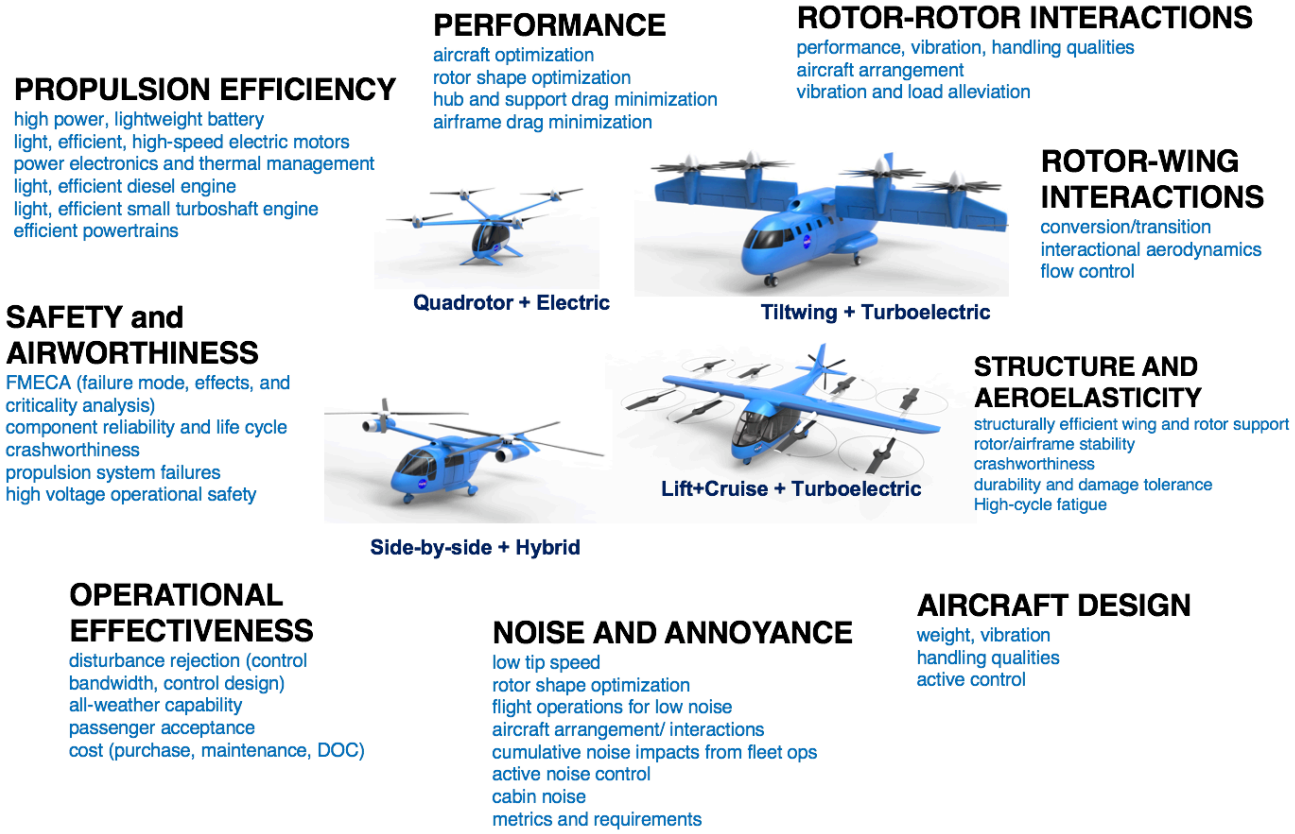

Figure 21. Research areas for Urban Air Mobility.

4) Silva, C.; Johnson, W.; Antcliff, K.R.; and Patterson, M.D. "VTOL Urban Air Mobility Concept Vehicles for Technology Development." AIAA Paper No. 2018-3847, June 2018.

5) Johnson, W. "NDARC. NASA Design and Analysis of Rotorcraft." NASA TP 2015-218751, April 2015.

6) Johnson, W. "NDARC — NASA Design and Analysis of Rotorcraft. Theoretical Basis and Architecture." American Helicopter Society Specialists' Conference on Aeromechanics, San Francisco, CA, January 2010.

7) Johnson, W. "NDARC — NASA Design and Analysis of Rotorcraft. Validation and Demonstration." American Helicopter Society Specialists' Conference on Aeromechanics, San Francisco, CA, January 2010.

8) Johnson, W. "Propulsion System Models for Rotorcraft Conceptual Design." American Helicopter Society 5th Decennial Aeromechanics Specialists' Conference, San Francisco, CA, January 2014.

9) Meyn, L.A. "Rotorcraft Optimization Tools: Incorporating Rotorcraft Design codes into Multi-Disciplinary Design, Analysis, and Optimization." American Helicopter Society Technical Conference on Aeromechanics Design for Transformative Vertical Flight, San Francisco, CA, January 2018.

10) Boyd, D.D., Jr.; Greenwood, E.; Watts, M.E.; and Lopes, L.V. "Examination of a Rotorcraft Noise Prediction Method and Comparison to Flight Test Data." NASA TM 2017-219370, January 2017.

11) Krishnamurthy, S.; Rizzi, S.A.; Boyd, D.D., Jr.; and Aumann, A.R. "Auralization of Rotorcraft Periodic Flyover Noise from Design Predictions." American Helicopter Society 74th Annual Forum, Phoenix, AZ, May 2018.

12) Snyder, C.A., and Thurman, D.R. "Effects of Gas Turbine Component Performance on Engine and Rotary Wing Vehicle Size and Performance." American Helicopter Society 66th Annual Forum, Phoenix, AZ, May 2010.

13) Lawrence, B.; Theodore, C.R.; Johnson, W.; and Berger, T. "A Handling Qualities Analysis Tool for Rotorcraft Conceptual Designs." The Aeronautical Journal, 122:1252 (June 2018).

14) Rohl, P.J.; Dorman, P.; Cesnik, C.E.S.; and Kumar, D. "IXGEN — A Modeling Tool for the Preliminary Design of Composite Rotor Blades." American Helicopter Society Future Vertical Lift Aircraft Design Conference, San Francisco, CA, January 2012.

15) Hahn, A. “Vehicle Sketch Pad: Parametric Geometry for Conceptual Aircraft Design.” AIAA Paper No 2010-657, January 2010.

16) Perry, T., and Gallaher, A. “Automated Layout with a Python Integrated NDARC Environment.” American Helicopter Society 74th Annual Forum, Phoenix, AZ, May 2018.

17) Johnson, W. “Rotorcraft Aeromechanics Applications of a Comprehensive Analysis.” HeliJapan 1998: AHS International Meeting on Rotorcraft Technology and Disaster Relief, Gifu, Japan, April 1998.

18) Johnson, W. “CAMRAD II, Comprehensive Analytical Model of Rotorcraft Aerodynamics and Dynamics, Manuals.” Johnson Aeronautics, 2017.

19) Johnson, W. *Rotorcraft Aeromechanics*. New York: Cambridge University Press, 2013 (section 18.5.6).

NOMENCLATURE

ATR	average temperature response
CFR	code of federal regulations
DGW	design gross weight
ETS	emissions trading scheme
HECTR	high efficiency civil tilt rotor
IRP	intermediate rated power (typically 30 min)
ISA	international standard atmosphere
MCP	maximum continuous power
MRP	maximum rated power (typically 10 min)
RVLT	Revolutionary Vertical Lift Technology
SLS	sea-level standard
TRL	technology readiness level
VTOL	vertical take-off and landing

A	rotor disk area, πR^2
A_{blade}	total blade area
C	charge capacity (Wh or MJ)
C_T	rotor thrust coefficient, $T/\rho A V_{tip}^2$
C_W	aircraft weight coefficient, $W/\rho A V_{tip}^2$
D	rotor diameter, $2R$
D/q	drag divided by dynamic pressure
DL	disk loading, GW divided by total rotor disk area
FM	aircraft or rotor figure of merit
GW	gross weight (WO + payload + fuel)
I	current, $I = xC$
L	rotor lift
L/D_e	aircraft effective lift-to-drag ratio, WV/P
L/D_e	rotor effective lift-to-drag ratio, $LV/(P_o+P_i)$
P	power
P_o	profile power
P_i	induced power
R	rotor blade radius; range
T	rotor thrust
V	speed
V_{be}	best endurance speed (maximum 1/fuelflow)
V_{br}	best range speed (99% high side max V/fuelflow)
V_{cruise}	cruise speed
V_{tip}	rotor tip speed
W	weight
WE	aircraft empty weight
WO	operating weight (WE + fixed useful load)
x	current (capacity per hour)
ρ	air density
σ	rotor solidity, A_{blade}/A